Military Technical College
Kobry Elkobbah,
Cairo, Egypt

2nd International Conference on
Electrical Engineering
ICEENG 99

ADAPTIVE SPACE–TIME SIDELOBE CANCELLER

SALEM* I., HANAFY ** A., HUSSEIN*** H.G. and MOUFID **** A. D.

ABSTRACT

Classical adaptive sidelobe canceller (CASLC) schemes which use only complex spatial weights are inherently narrowband, and consequently perform poorly when attempting to suppress wideband interference. This paper presents a novel solution to this problem by using tapped delay line filters in each spatial auxiliary channel, and utilizing the adaptive space-time processing for performing the required null. This sidelobe canceller is referred to as adaptive space–time sidelobe canceller "ASTSLC". The higher performance achieved by the ASTSLC architecture comes at the cost of a considerable increase in its complexity. ASTSLC technique can be used for compensation due to bandwidth degradations, channel mismatching, and multipath phenomena. In this work, the problem of bandwidth compensation is considered. The objective of our analysis is to develop some insight into the way in which space–time processing leads to performance improvement as compared to the CASLC. Moreover, some quantitative estimates of how the performance varies with array antenna (space processing) and transversal filter (time processing) parameters are also investigated and presented.

KEYWORDS

Sidelobe cancelle, Adaptive, Interference, Tapped delay lines, Transversal filter, Space-time processing, Bandwidth compensation, Estimation

---

* Professor, Egyptian Armed Forces
** Professor, Egyptian Armed Forces
*** Doctor, Egyptian Armed Forces
**** Ph.D. Student, Syrian Armed Forces

1. INTRODUCTION

Performance of interference rejection by a classical adaptive "SLC" has been discussed mostly for the case of a monochromatic undesired signal (narrowband), where a simple and sharp null in the adaptive beam pattern is enough for rejection [1-4]. If the interference is wideband as usually in case of jamming, CASLC system tends to gather as many nulls of its pattern as possible in the neighborhood of center frequency of the interference. This leads to attain a certain level of rejection (cancellation ratio) over the interference band. In this case, much longer time for adaptation is required. Moreover, if the jamming frequency hops randomly, the system falls in the everlasting game of hunting, and the output remains unsatisfactory level. This paper presents a solution to this problem by using tapped delay line filters in each spatial auxiliary channel. This adaptive SLC is referred to as ASTSLC. This technique can be applied to compensate for degradations due to bandwidth, channel mismatching, and multipath phenomena. Problem of multipath has been widely discussed in [5,6]. In this paper, the problem of bandwidth compensation effects has been considered to investigate and evaluate the performance of the ASTSLC.
A broadband interference source can be considered as sum of several narrowband interference sources located at different spatial locations. Using a complex–valued weight, appropriate for one frequency, f_1 (narrowband case), will not be appropriate for other frequency, f_2. This is because the array patterns nulls shift as the value of the frequency changes. This leads to the conclusion that different complex–valued weights are required at different frequencies if an array null is to be maintained in the same direction for all frequencies of interest. A simple and effective way of obtaining different amplitude and phase weights at a number of frequencies over the band of interest is to use a tapped delay line filter (transversal filter) in each spatial auxiliary channel. Therefor, the higher performance provided by the ASTSLC architecture comes at the cost of a considerable increase in its complexity.

2. CONFIGURATION OF ASTSLC SYSTEM

The adaptive space–time sidelobe canceller architecture is shown in Fig.1. It consists of a high–gain main antenna (N_1 -elements) and auxiliary antenna (N_2-elements). The transversal filter in each auxiliary element can be realized by tapped delay line having "L" complex weights. A tapped delay line has a periodic frequency response with a period equal to "$1/\Delta$" along the frequency axis. If the tap spacing "Δ" is sufficiently small and the number of "L" taps is large (the frequency resolution of the filter is $(1/L\Delta)$, this network controls the gain and the phase at each frequency component within the band of interest. An upper limit on the tap spacing is given by the desired array cancellation bandwidth "B" as $B \leq 1/\Delta$ [7]. The adaptive tapped delay line architecture required to perform ASTSLC is shown in Fig. 1. The adaptive weights "W" are applied at each tap in each spatial auxiliary channel prior to the final beamforming summation of sidelobes. For "N_2" auxiliary spatial channels with "L" taps per channel, the total number of adaptive weights to be calculated is "$N_2 L$".

The main antenna consists of "N_1" isotropic elements with non-adaptive weights. These weights may have a tapering distribution according to the required sidelobe level. A taped delay of value $D=(L-1)\Delta/2$ is included in the main channel. This delay represents the center tap of the auxiliary to permit a compensation for both positive and negative values of the off-broadside angle θ.

3. OPTIMAL WEIGHT SOLUTION

Throughout the analysis in this paper, the superscripts T, H, and $\cdot$ will denote transpose, complex conjugate transpose (Hermitian transpose), and complex conjugate operations, respectively. Denote $\underline{\tilde{u}}$ as a column vector of a dimension (LN_2+1) which represents the snapshot of the array antennas. This vector is given by

$$\underline{\tilde{u}} = \begin{bmatrix} b \\ \underline{u} \end{bmatrix} \tag{1}$$

Where "b "denotes the main antenna output, and

$$\underline{u} = \begin{bmatrix} \underline{u}_1 \\ \underline{u}_1 \\ . \\ . \\ \underline{u}_{N_2} \end{bmatrix} \tag{2}$$

Where,

$$\begin{aligned} \underline{u}_1 &= [u_{11} u_{12} \ldots\ldots u_{1L}]^T \\ \underline{u}_2 &= [u_{21} u_{22} \ldots\ldots u_{2L}]^T \\ &. \\ &. \\ \underline{u}_{N_2} &= [u_{N_2 1} u_{N_2 2} \ldots\ldots u_{N_2 L}]^T \end{aligned} \tag{3}$$

Where,

$$u_{ij} = u_j[t-(i-1)\Delta] \tag{4}$$

$i = 1,2,\ldots, L$

$j = 1,2,\ldots, N_2$

It is seen that each vector has a dimension of (LX1). In an exactly similar manner, the weight vector can be given by

$$\underline{W} = \begin{bmatrix} \underline{w}_1 \\ \underline{w}_2 \\ . \\ . \\ \underline{w}_{N_2} \end{bmatrix} \tag{5}$$

Where,

$$\begin{aligned} \underline{w}_1 &= \begin{bmatrix} w_{11} & w_{12} & \cdots & w_{1L} \end{bmatrix}^T \\ \underline{w}_2 &= \begin{bmatrix} w_{21} & w_{22} & \cdots & w_{2L} \end{bmatrix}^T \\ &. \\ &. \\ \underline{w}_{N_2} &= \begin{bmatrix} w_{N_2 1} & w_{N_2 2} & \cdots & w_{N_2 L} \end{bmatrix}^T \end{aligned} \tag{6}$$

It is seen that the weight vector $\underline{W}$ has a dimension of N_2L. The weight vector for the snapshots is defined as

$$\underline{\tilde{w}} = \begin{bmatrix} b \\ -\underline{w} \end{bmatrix} \tag{7}$$

The ASTSLC system output is defined as the residue

$$\begin{aligned} \varepsilon &= \underline{\tilde{w}}^H \, \underline{\tilde{u}} \\ &= b - \underline{w}^H \, \underline{u} \end{aligned} \tag{8}$$

3.1 Derivation

Each snapshot of the array antenna has three contributions: the signal S, the interference I, and the white noise N,

$$\underline{\tilde{u}} = \underline{\tilde{u}}_S + \underline{\tilde{u}}_I + \underline{\tilde{u}}_N \tag{9}$$

The objective of sidelobe cancellation is to construct a weight vector for the auxiliary antennas to minimize the interference power in the residue ε. The optimal weight vector is given by the Wiener solution [8]

$$W_O = R_{uu}^{-1} \underline{r}_{ub} \tag{10}$$

Where R_{uu} is the covariance matrix of the outputs of the auxiliary antenna for the entire auxiliary multichannel processor when the signal is absent, and $\underline{r}_{ub}$ is the cross correlation vector between the main antenna and the auxiliary antenna outputs. In the derivation of (10), it has been assumed that (i) the signal, interference, and white noise are mutually uncorrelated and (ii) R is nonsingular so that R^{-1} exists. Then LN_2-th components of $\underline{r}_{ub}$ measure the correlation between the outputs of the main antenna and the LN_2-th auxiliary elements for the entire auxiliary multichannel processor. To calculate the Wiener solution, both R_{uu} and $\underline{r}_{ub}$ must be known. In practice, they have to be estimated from the outputs of the main and auxiliary channels.

Let $\underline{\tilde{u}}_1, \underline{\tilde{u}}_2, \ldots\ldots, \underline{\tilde{u}}_M$ be a set of M snapshots taken in the absence of the signal. The sample matrix inversion (SMI) method estimates W_o with the equation [9]

$$\hat{W}_O = \hat{R}_{uu}^{-1} \hat{\underline{r}}_{ub} \tag{11}$$

Where

$$\hat{R}_{uu} = UU^H \tag{12}$$

is the sample covariance matrix, $U = \left(\underline{\tilde{u}}_1, \underline{\tilde{u}}_2, \ldots\ldots, \underline{\tilde{u}}_M\right)$ is the matrix of auxiliary channels outputs,

$$\hat{\underline{r}}_{ub} = U\underline{b}^* \tag{13}$$

is the sample correlation vector, and $\underline{b} = \left(b_1, b_2, \ldots\ldots, b_M\right)^T$ is the vector for the main antenna outputs.

The above equation (13) suggest that there is a more general approach to construct an adaptive weight vector for the auxiliary channels, i.e. identify this vector as a solution of the equation

$$U^H \mathbf{W} = \underline{b}^* \tag{14}$$

Or, equivalently, the system of linear equations

$$\underline{\tilde{u}}_m^H \mathbf{W} = b_m^* \qquad (15)$$

$$m=1,2, \ldots, M.$$

The benefit of using the adaptive sidelobe cancellation "ASLC" can be measured by introducing the interference cancellation ratio (CR), defined as the ratio of the output noise power without and with the auxiliary array [6]:

$$CR = \frac{E\{|b|^2\}}{E\{|b - \hat{W}^T \underline{\tilde{u}}|\}} = \frac{E\{|b|^2\}}{E\{|b|^2\} - \underline{r}_{ub}^H R_{uu}^{-1} \underline{r}_{ub}} \qquad (16)$$

4. SIMULATION RESULTS

Presented here are examples, which demonstrate that the weight-vector construction method indeed produces adapted beam patterns with interference suppression properties. The antenna system is shown in Fig.1. It consists of a linear array with N= (N_1+N_2) isotropic elements spaced at distance of half a wavelength, i.e. d= 0.5λ, where d is the element spacing and λ is the signal wavelength. The outputs of the first N_1 elements are weighted with a Tschebyscheff window and summed to produce the main antenna output. The (k+N_1)-th element is identified as the k-th auxiliary antenna (k=1,2, ..., N_2). The outputs of the isotropic antennas are calculated as

$$u_{n'} = \sum_{j=1}^{J} \sqrt{p_j}\ e^{i\phi_j}\ e^{i\pi(1+B/fo)\, n' \sin\theta_j} + \eta_{n'} \qquad (17)$$

$$n' = 1,2, \ldots, N'.$$

Here, B is the interference signal bandwidth, fo is the carrier frequency of the radar system, J is the number of interference sources, j is the interference identification number, p_j is the output power due to the j-th source, ϕ_j is a random phase, λ_j is the interference source wavelength, θ_j is the interference bearing measured clockwise from the foresight direction, and $\eta_{n'}$ is the white noise amplitude. This amplitude is calculated with mean and variance given by

$$E\{Re(\eta_{k'})\} = E\{Im(\eta_{k'})\} = 0 \tag{18}$$

And

$$var\{Re(\eta_{k'})\} = var\{Im(\eta_{k'})\}$$

Where σ^2 is the expected value of white noise power at the output of the individual antennas. The main antenna output is calculated as

$$b = \sum_{k'=1}^{N_1} \alpha_{k'} u_{k'} \tag{20}$$

Where $\alpha_{k'}$ is the window coefficients [10].

The gain pattern is defined as

$$G(\theta) = -\frac{\left| s_o(\theta) - \underline{W}^H \underline{s}(\theta) \right|^2}{\sum_{k'=1}^{N_1} |\alpha_{k'}|^2 + |\underline{W}|^2} \tag{21}$$

Where

$$s_o(\theta) = \sum_{k'=1}^{N_1} \alpha_{k'} e^{j\pi k' \sin\theta} \tag{22}$$

And

$$s_k(\theta) = e^{j\pi(k+N_1)\sin\theta} \tag{23}$$

$$k=1,2, \ldots, LN_2$$

Are the outputs of the main and auxiliary antennas due to a unit output amplitude signal at bearing θ_s. The denominator in (21) is a scale factor such that the expected value of G (θ) due to white noise is equal to σ^2.

A set of simulation examples has been carried out to investigate and evaluate the performance of the proposed technique. Fig. 2 shows the effect of bandwidth of the with N_1=21, N_2=2, the incident angle of the interference at 30°, INR=30 dB and L=1. As it is clear from the figure, the cancellation ratio decreases as the normalized

bandwidth of interference "B/fo" increases. Also, for small values of the normalized bandwidth (0.01< B/fo <0.05), high CR is obtained. This is due the fact that the interference can be considered as narrowband. Therefore, additional degree of freedom is required to compensate for the effects of the interference bandwidth. Using the time processing, bandwidth effects can be compensated. Fig. 3 illustrates a plot of CR as a function of number of weights (snapshots) for two values of interference incident angles. The other simulation parameters are shown on the figure. As we expected, using the time processing, additional increase in the CR is obtained at B/fo=0.1(CR=9 dB as compared to the narrowband array of Fig. 2). Moreover, the CR is very sensitive to the interference incident angle as it is clear form the figure (θ_j =30° and θ_j =35°). There are also an optimum number of taps after which the improvement in the CR is not significant. In our case of simulation, four taps is enough to achieve CR=22 dB at θ_j =30°. Better CR is obtained at θ_j =35° as compared to θ_j =30°. This is due to the fact that the closer the interference angle to the desired target direction (θ_s =0°) the lower values of the CR are obtained. Other important features of the ASTSLC are investigated and presented in Fig.4. This includes the dependence of the cancellation ratio on the time-bandwidth product "ΔB" for several number of taps "L". For narrowband SLC (L=1), the cancellation ratio is independent on "ΔB". In this case, less CR is obtained for broadband interference (CR=9 dB vs. CR=22 dB). On the other hand, for broadband SLC, strong dependence of the CR on "ΔB" is obtained (L=1, 2, 3, 4 and 5). Finally, a case study of a broadband interference is assumed, and the result of simulation is presented in Figs. 5 and 6. The data for simulation are shown on the figures. The objective is to show how the ASTSLC performs bandwidth compensation. The main and adaptive beam patterns are given in Fig.5. In this figure, the ASTSLC places a null at the required angle (θ_j =40°) as compared to the CASLC where the null is placed at different angle due to the bandwidth effects. A detailed plot is shown in Fig.6 to illustrate how the compensation process toke place as function of the time-bandwidth product for the same case of study presented in Fig.5. This figure represents a zooming plot for the adaptive patterns at the neighborhood of the required null. As it is clear from the figure, three taps are required for compensating the shift in the null of the interference signal. The effect of the bandwidth product "ΔB" has the dominant impact on placing the null at the right direction. In our simulation, two values are assumed (ΔB=0.14and ΔB 0.28). As it is clear from the Figure, ΔB=0.28 is the estimated value to place the null at θ_j=40°. This is perfectly conside with the case of NB array. In conclusion, the ASTSLC has better performance as compared to the CASLC for either narrowband or broadband interference.

5. CONCLUSION

Computer code has been developed to simulate the ASTSLC. The objective is to investigate the performance of the ASTSLC as compared to the CASLC assuming broadband interference sources. The results of simulation show that the ASTSLC is an excellent approach for bandwidth compensation. Problem of mismatching and multipath in case of broadband interference will be considered in future work.

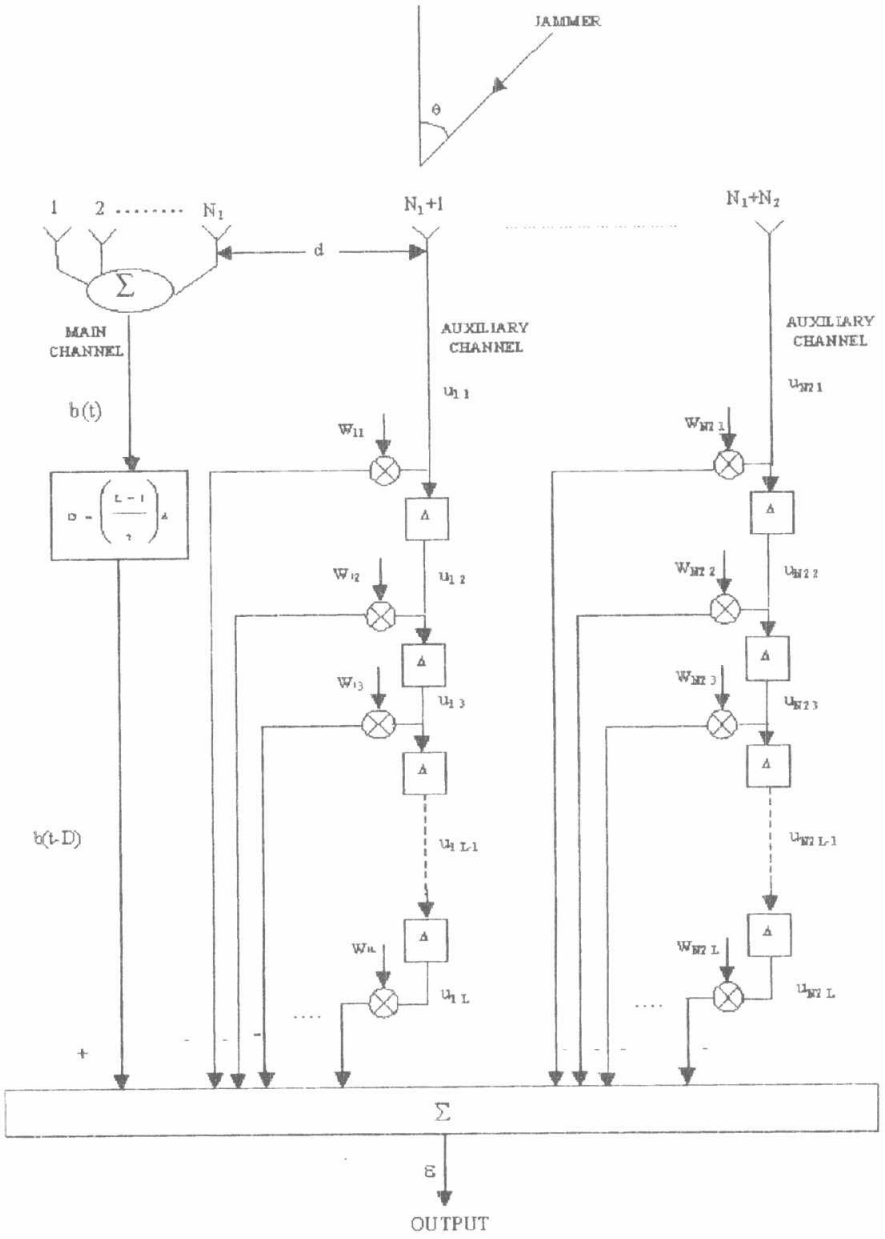

Fig.1 The ASTSLC scheme with main channels and tapped delay line auxiliary Channels for bandwidth compensation

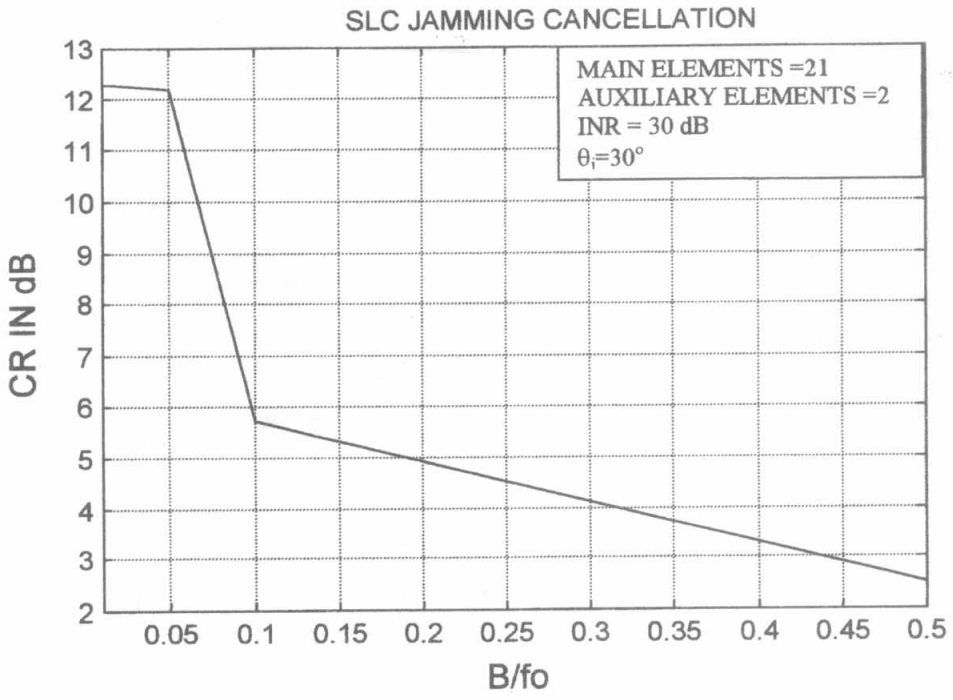

Fig.2 Interference bandwidth effect on the CR of CASLC

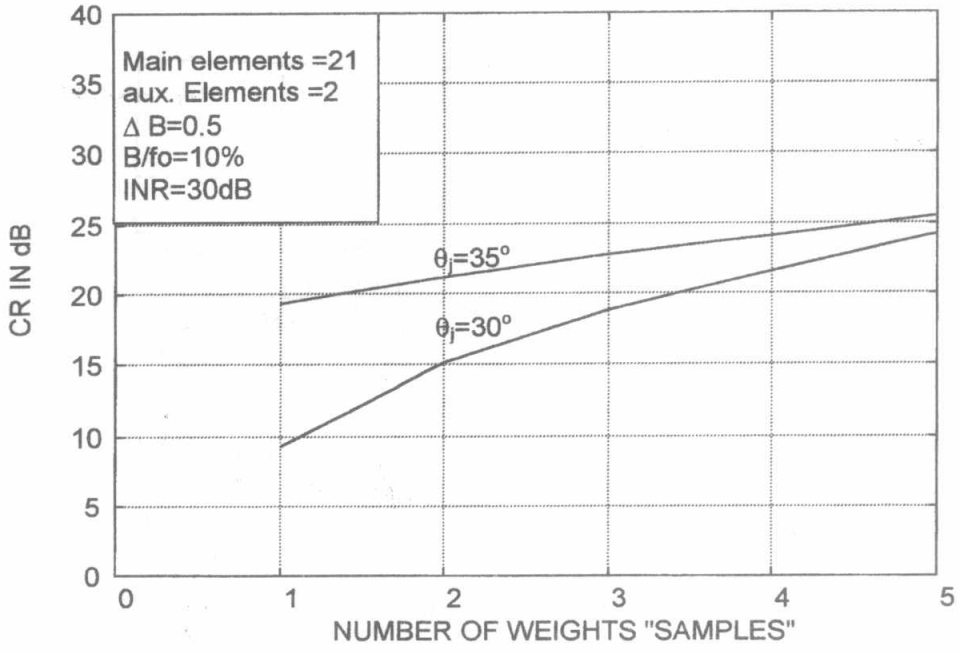

Fig. 3 Cancellation Ratio of ASTSLC versus number of snapshots for two different jammer angle (θ_j)

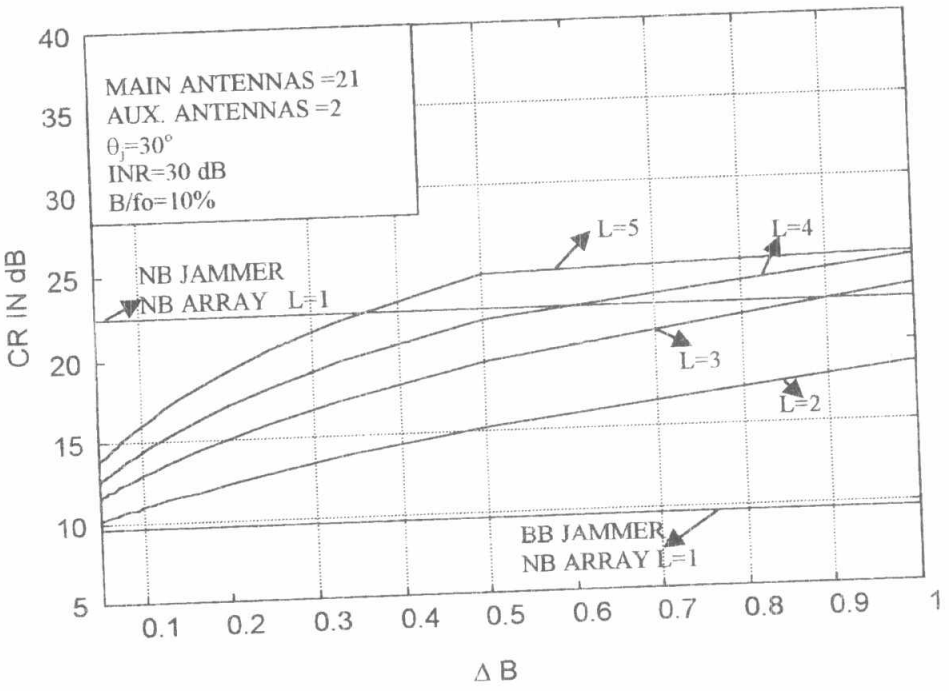

Fig. 4 Cancellation Ratio versus ΔB for narrowband (NB) and broadband (BB) interferences sources.

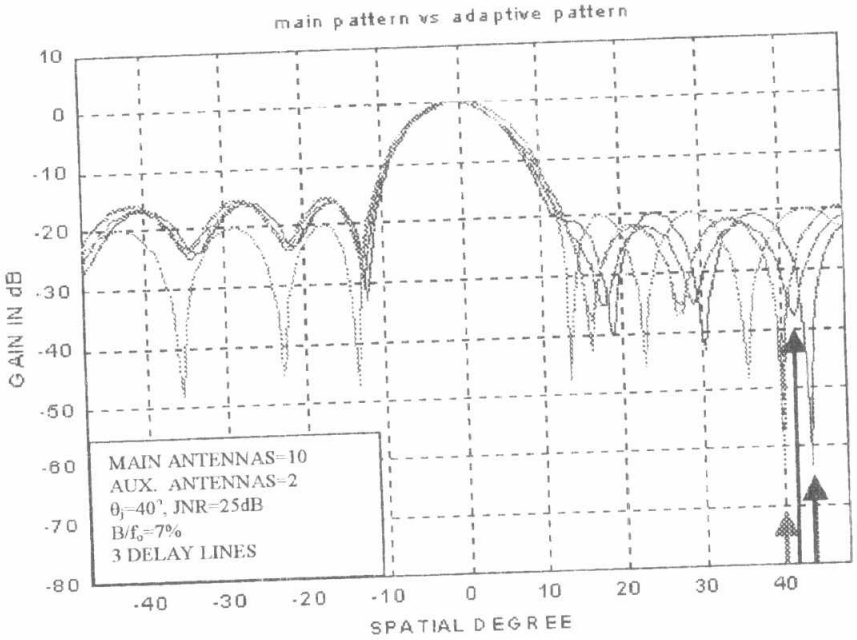

Fig. 5 Adaptive beam patterns and quiescent pattern of ASTSLC and CASLC, in case of NB and BB jammers.

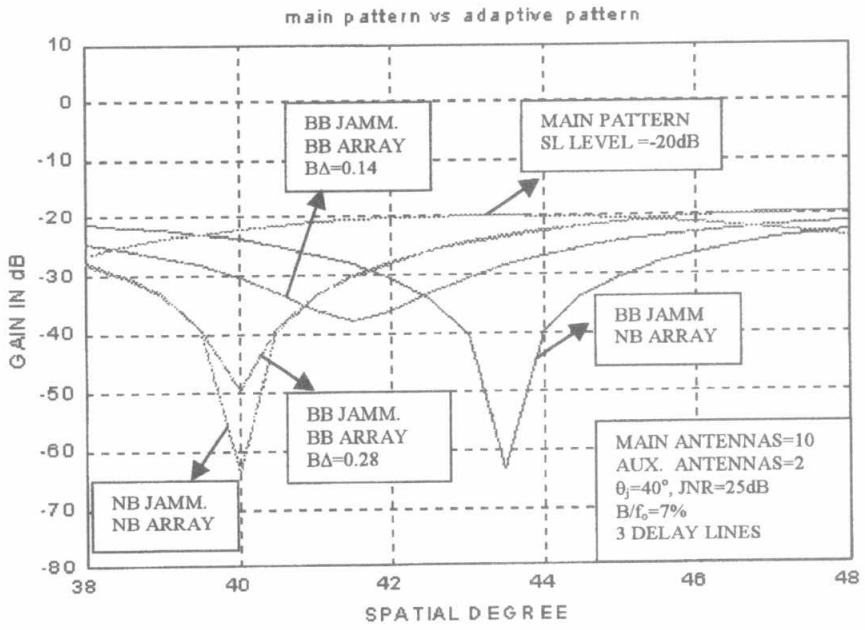

Fig. 6 A zooming plot of Fig.5 neighborhood the direction of the interference in range of (38-48) degrees.

6. REFERENCES

[1] S. Haykin and A. Steinhardt, "Adaptive radar detection and estimation," John Wiley & Sons. Inc. 1992.

[2] R. Nitzberg, "Adaptive signal processing for radar," Artech House, Inc. 1992.

[3] Stanley M. Yuen, "Algorithmic, Architectural, and beam pattern issues of sidelobe cancellation," IEEE Trans. On Aerospace and Electronic Systems vol. 2, pp. 459-471 July 1989.

[4] Eric K. L. Hung, " Adaptive sidelobe cancellation by linear prediction," IEEE International Radar Conference pp. 286-291 Canadian Cowns 1985.

[5] R.A. Monzingo and T.W. Miller, "Introduction to Adaptive Arrays", Wiley, New York, 1980.

[6] D. R. Morgan and A. Aridgides, "Adaptive sidelobe cancellation wide-band multipath interference," IEEE Trans. Antennas Propagat. , Vol. AP-33, pp. 908- 917, Aug. 1985.

[7] A. Farina, "Antenna-based signal processing techniques for radar systems", Artech House, Inc. 1992.

[8] B. Widrow and S. D. Stearns, "Adaptive signal processing", Prentice-Hall, Inc. 1985.

[9] Reed, I. S. Mallett, J. D., and Brennan, L. E., "Rapid convergence rate in adaptive arrays", IEEE Trans. On Aerospace and Electronic System, AES-9, pp. 853-863. Nov. 1974.

[10]Constantine A. Balanis, "Antenna Theory", John Wily & Sons 1997.